Statistical and phase properties of displaced Kerr states

A. D. Wilson-Gordon,* V. Bužek,† and P. L. Knight
Optics Section, Blackett Laboratory, Imperial College, London SW7 2BZ, England
(Received 1 July 1991)

We study the statistical and phase properties of the output states of a Mach-Zehnder interferometer with a nonlinear Kerr medium in one of its arms. The combination of nonlinearity and displacement produced by the interferometer generates output states (displaced Kerr states) that, unlike those derived from a Kerr medium alone (Kerr states), do not necessarily retain the photon statistics of the initially coherent field. As the parameter characterizing the nonlinear medium is varied, the statistics of the output field vary from sub-Poissonian to super-Poissonian. The photon-number distributions of these states are rationalized by examining their quasiprobability distributions, which vary from banana-shaped for sub-Poissonian statistics to complicated interference structures for highly super-Poissonian statistics. The number-phase properties of the Kerr and displaced Kerr states are studied for the case of small photon numbers (relevant to cavity quantum electrodynamics) using a methodology based on the Pegg-Barnett formalism. In particular, we determine the range of parameters for which the states are minimum-uncertainty states and whether they are squeezed with respect to photon number and phase, drawing a distinction between a sub-Poissonian nature and number squeezing. Finally, we find that sub-Poissonian statistics can coexist with quadrature squeezing for a range of parameters.

PACS number(s): 42.50.Dv, 42.65.−k

I. INTRODUCTION

Nonlinear-optical interactions have been employed widely to generate nonclassical light such as squeezed or sub-Poissonian light [1–5]. One of the simplest nonlinearities is the purely dispersive optical Kerr effect, in which a nonlinear refractive index modifies the phase-sensitive quantum noise of an input field [6]. The Kerr effect generates quadrature squeezing but does *not* modify the input field photon statistics, which remain Poissonian for a coherent input [7]. A number of authors have discussed how the Kerr effect, while preserving the photon statistics, can generate from an initially coherent input an output which is a macroscopic superposition of distinguishable states [8–12] of great interest in current debates on quantum measurement theory [13]. The generation of such superpositions is graphically portrayed by a study of the bifurcations of phase-space quasiprobabilities such as the Husimi Q function or the Wigner function [14]. The curious preservation of the photon statistics by the Kerr effect and the retention of purely Poissonian photon-number fluctuations is connected with the action of the Kerr field self-coupling on the relative phases of states of differing quantum numbers; this phase modification is of course precisely that needed for quadrature squeezing. To see modifications in the photon-number fluctuations after a Kerr interaction it is necessary to displace the Kerr state (the state generated from an initially coherent state by a Kerr interaction) in phase space. The incorporation of a Kerr interaction in one arm of a nonlinear Mach-Zehnder interferometer (Fig. 1) will establish this necessary combination of nonlinearity *and* displacement [15–20]. We study in this paper the quantum fluctuations of such a displaced Kerr state. In particular we investigate the "squeezing" of number and phase fluctuations and to do so pay particular attention to a careful definition of squeezing in this context. In most previous work on nonlinear Mach-Zehnder interferometers, it is assumed that very large photon numbers are involved. Under these circumstances the number and phase uncertainties have an unambiguous semiclassical interpretation. But for small photon numbers the quantum nature of phase becomes very important and care needs to be taken to parametrize phase fluctuations and number-phase uncertainty relations appropriately [21–23]. It could be argued that it is purely academic to study the Kerr effect for a field with a small photon number, as one would anticipate large photon numbers being necessary to produce significant nonlinear phase shifts. This is true for most *optical* interactions, but is quite false for studies of nonlinearities in cavity quantum electrodynamics where nonlinearities due to optical Stark shifts have already been observed in micromasers [24–29] and have been proposed as ingredients for quantum nondemolition measurements based on the Kerr effect which is sufficiently large to produce observable phase shifts [30] for photon numbers $n \sim 1$. Under these circumstances purely semiclassical ideas of phase fluctuations are irrelevant. In the past, phase fluctuations in the nonlinear Mach-Zehnder interferometer have been described by the Susskind-Glogower phase operators [16,31,32]. The recently developed Hermitian phase operator of Pegg and Barnett [21–23] is, however, much more revealing about the nature of phase fluctuations and has already been applied in the study of Kerr states [12,33]. However, these previous studies have emphasized the traditional large-photon-number limit and have employed a continuous phase distribution function appropriate for such a limit; here of course the Susskind-Glogower [31] and Pegg-Barnett [21–23] approaches are in full agreement. But for $n \sim 1$, these approaches differ and great care must be taken to calculate phase variances for small photon numbers. The continuous phase distribution approximation is not justified. We adopt an appropriate methodology based on the Pegg-Barnett formalism, but emphasizing the proper phase distribution for states of small photon number.

In addition we propose appropriate measures of phase and number fluctuations to characterize whether output states are number-phase minimum-uncertainty states (MUS's), and whether such states are sub-Poissonian, and finally whether they are squeezed with respect to number and phase. We distinguish between number squeezing and a sub-Poissonian nature and link this behavior to quadrature squeezing.

The interferometer relevant to the production of displaced Kerr states [15–20] is shown in Fig. 1. In one arm of the device a nonlinear Kerr medium generates the appropriate intensity-dependent phase shifts through a coupling quadratic in the photon number:

$$\hat{H} = \hbar\omega\hat{a}^\dagger\hat{a} + \hbar\chi(\hat{a}^\dagger)^2(\hat{a})^2 , \tag{1}$$

where the nonlinear coupling coefficient χ is related to the value of the Kerr medium third-order susceptibility. The input state to the Kerr medium is a coherent state $|\alpha\rangle$ derived from the beam-splitter transformations [34] modified by the transmissivity of the input beam splitter and the associated vacuum state of the second input port. The output state from the Kerr medium [16] is

$$|\psi_K\rangle = \hat{U}_K(\gamma)|\alpha\rangle , \tag{2}$$

where $U_K(\gamma)$ is the evolution operator

$$\mathbf{U}_K(\gamma) = \exp\left[\frac{i}{2}\gamma\hat{n}(\hat{n}-1)\right] , \tag{3}$$

with $\gamma \equiv 2\chi L/v$, where L is the length of the Kerr medium and v the appropriate phase velocity inside the medium. The second beam splitter combines the Kerr state with the coherent state of the second arm of the interferometer, and this combination acts to *displace* the Kerr state to give a final output state

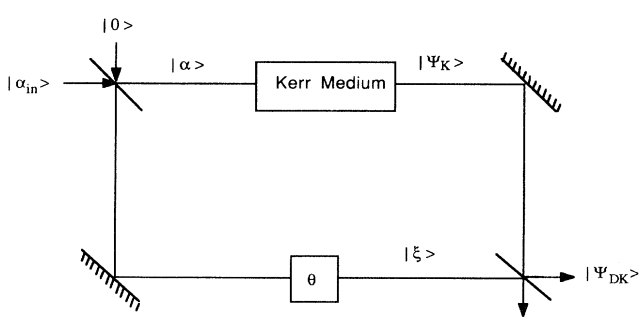

FIG. 1. Schematic diagram of a nonlinear Mach-Zehnder interferometer: coherent and vacuum field inputs $|\alpha_{\text{in}}\rangle$ and $|0\rangle$ are superposed, and in one arm transformed by propagation through a Kerr medium while in the other arm a phase shift θ is imposed.

$$|\psi_{DK}\rangle = \hat{D}(\xi)|\psi_K\rangle , \tag{4}$$

where $\hat{D}(\xi)$ is the Glauber displacement operator [14]

$$\hat{D}(\xi) \equiv \exp(\xi\hat{a}^\dagger - \xi^*\hat{a}) . \tag{5}$$

In this way we see that the nonlinear Mach-Zehnder interferometer combines a nonlinear Kerr transformation with a displacement in phase space.

In Sec. II, we construct the Kerr $|\psi_K\rangle$ and displaced Kerr states $|\psi_{DK}\rangle$ and calculate the Mandel Q parameter as a function of γ for the displaced Kerr states. The photon-number probability distributions for various values of γ are also discussed. The quasiprobability functions are calculated in Sec. III for the same values of γ as in Sec. II, and the connection between photon-number probability distributions and quasiprobability functions is shown. The phase properties of the states are presented in Sec. IV. The quadrature squeezing properties are discussed in Sec. V, and conclusions are drawn in Sec. VI.

II. KERR AND DISPLACED KERR STATES

A. Kerr states

The Kerr states defined in Eq. (2) can be written in a number-state basis as

$$|\psi_K\rangle = e^{-(1/2)|\alpha|^2} \sum_{n=0}^{\infty} \frac{\alpha^n}{n!^{1/2}} e^{i(1/2)\gamma n(n-1)}|n\rangle \equiv \sum_{n=1}^{\infty} q_n|n\rangle , \tag{6}$$

where the coherent state $|\alpha\rangle$ is expressed as

$$|\alpha\rangle = e^{-(1/2)|\alpha|^2} \sum_{n=0}^{\infty} \frac{\alpha^n}{n!^{1/2}}|n\rangle \equiv \sum_{n=0}^{\infty} r_n|n\rangle . \tag{7}$$

The photon-number distribution

$$P_n = |\langle n|\psi_K\rangle|^2 = |q_n|^2 \tag{8}$$

for the Kerr state is identical to that of the coherent state because the probability amplitudes q_n and r_n differ only by a phase factor. The Kerr state will exhibit Poissonian photon statistics and its Mandel Q parameter [5], defined by

$$Q = (\langle\Delta\hat{n}^2\rangle - \langle\hat{n}\rangle)/\langle\hat{n}\rangle , \tag{9}$$

will be identically zero.

B. Displaced Kerr states

The displacement of the Kerr states by the unitary transformation

$$\hat{D}(\xi) = \exp(\xi\hat{a}^\dagger - \xi^*\hat{a}) \tag{10}$$

gives the displaced Kerr states

$$|\psi_{DK}\rangle = \hat{D}(\xi)|\psi_K\rangle \equiv \sum_{n=0}^{\infty} c_n|n\rangle , \tag{11}$$

which may have varying degrees of sub-Poissonian

($Q<0$) or super-Poissonian ($Q>0$) statistics depending on the values of the parameters α, ξ, and γ. Combining Eqs. (6) and (11), we find that the probability amplitudes c_n are given by

$$c_n=\sum_{m=0}^{\infty} q_m \langle n|\hat{D}(\xi)|m\rangle \ , \tag{12}$$

where the states

$$|\xi,m\rangle \equiv D(\xi)|m\rangle \tag{13}$$

are the displaced number states [35,36]. Then writing

$$|m\rangle=\frac{(a^{\dagger})^m|0\rangle}{m!^{1/2}} \tag{14}$$

and invoking the unitarity of $D(\xi)$ and its well-known translation properties

$$\hat{D}(\xi)\hat{a}^{\dagger}\hat{D}^{\dagger}(\xi)=\hat{a}^{\dagger}-\xi^* \ , \tag{15}$$

$$\hat{D}(\xi)|0\rangle=|\xi\rangle \ , \tag{16}$$

we obtain

$$\langle n|\hat{D}(\xi)|m\rangle=\sum_{k=0}^{m}(-\xi^*)^{m-k}\begin{bmatrix} m \\ k\end{bmatrix}\frac{\langle n|(a^{\dagger})^k|\xi\rangle}{m!^{1/2}} \ , \tag{17}$$

and because

$$\langle n|(a^{\dagger})^k=\begin{cases}\langle n-k|\left[\dfrac{n!}{n-k!}\right]^{1/2}, & k\le n \\ 0, & k>n \ ,\end{cases} \tag{18}$$

we obtain

$$\langle n|\hat{D}(\xi)|m\rangle = e^{-(1/2)|\xi|^2}\sum_{k=0}^{\min\{m,n\}}(-1)^{m-k} \times\frac{m!^{1/2}n!^{1/2}}{(m-k)!(n-k)!k!} \times|\xi|^{n+m-2k}e^{i\phi_\xi(n-m)} \ , \tag{19}$$

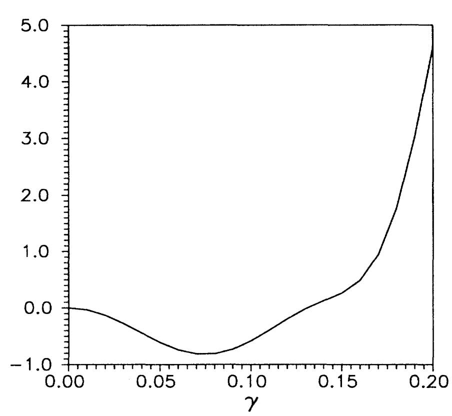

FIG. 2. Mandel's Q parameter vs γ for a displaced Kerr state with $|\alpha|=4$, $|\xi|=2$, and $\phi_\alpha=\phi_\xi=0$. The photon statistics are sub-Poissonian for $\gamma<0.13$ and super-Poissonian for $\gamma>0.13$. The minimum value of Q is -0.8 for $\gamma\simeq0.08$.

where $\xi=|\xi|\exp(i\phi_\xi)$. Finally on insertion of Eq. (19) into (12) we find

$$c_n=e^{-(1/2)(|\alpha|^2+|\xi|^2)} \times\sum_{m=0}^{\infty}e^{i\phi_\alpha m}e^{i(1/2)\gamma m(m-1)}|\alpha|^m \times\sum_{k=0}^{\min\{m,n\}}(-1)^{m-k}\frac{n!^{1/2}}{k!(m-k)!(n-k)!} \times e^{i\phi_\xi(n-m)}|\xi|^{n+m-2k} \tag{20}$$

with $\alpha=|\alpha|\exp(i\phi_\alpha)$.

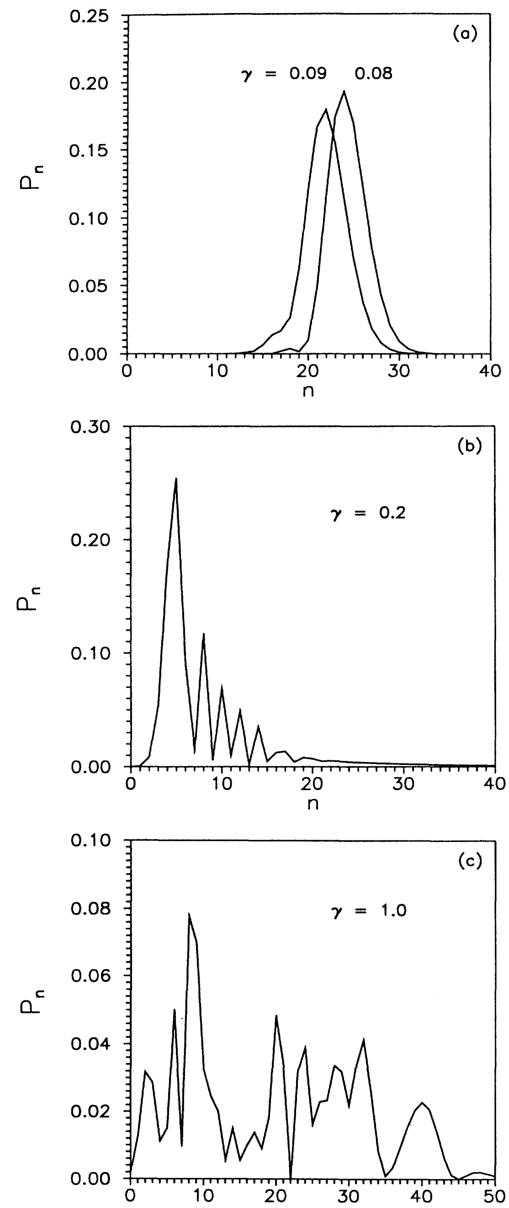

FIG. 3. Photon-number distribution for displaced Kerr states with (a) $\gamma=0.08$, 0.09; (b) $\gamma=0.2$, and (c) $\gamma=1.0$ corresponding to (a) sub-Poissonian and (b) and (c) super-Poissonian statistics. Other parameters are the same as in Fig. 2.

In order to determine the photon statistics of the displaced Kerr states, we calculated the photon-number distribution and the Mandel Q parameter of Eq. (9) using

$$\langle \hat{n} \rangle = \bar{n} = \sum_n nP_n \, ,$$
$$\langle \hat{n}^2 \rangle = \overline{n^2} = \sum_n n^2 P_n \, . \tag{21}$$

In Fig. 2 we plot Q as a function of γ for $|\alpha|=4$, $|\xi|=2$, and $\phi_\alpha=\phi_\xi=0$. We see that the displaced Kerr states for this particular value of $|\alpha|$ are sub-Poissonian for $\gamma \lesssim 0.13$ and super-Poissonian for $\gamma \gtrsim 0.13$ with the maximum degree of the sub-Poissonian statistics at $\gamma \simeq 0.08$ where $Q=-0.81$. We now plot in Fig. 3 the photon-number distributions for various values of γ that give sub-Poissonian and super-Poissonian statistics. Their behavior will be interpreted in Sec. III. In Fig. 3(a), we show P_n vs n for the state of a maximum sub-Poissonian nature (minimum value of Q) $\gamma=0.08$ and for a slightly less sub-Poissonian state $\gamma=0.09$. We see that the narrow peak for $\gamma=0.08$ is accompanied by a small satellite peak to lower n. For $\gamma=0.09$, the main peak is broader and the small peak appears as a shoulder. The case of super-Poisson statistics is shown in Figs. 3(b) and 3(c). In Fig. 3(b), $\gamma=0.2$ ($Q=4.8$) and there are a number of smaller peaks of decreasing intensity to the right of the main peak. This distribution is very similar to that of a "vertically" squeezed state with a large squeeze parameter with super-Poissonian statistics [2,37,38]. In Fig. 3(c), $\gamma=1.0$ and $Q=6.4$. Here the distribution has no discernible regularity. It should be noted that in the limit of small γ, $Q \to 0$ corresponding to a coherent state of mean photon number $\langle n \rangle = |\alpha+\xi|^2$ since $D(\xi)|\alpha\rangle = |\alpha+\xi\rangle \exp[-(\frac{1}{2})(\xi^*\alpha-\xi\alpha^*)]$.

III. QUASIPROBABILITY DISTRIBUTIONS

In this section, we present the quasiprobability distributions (QPD's) [14]

$$Q(\alpha') = \langle \alpha' | \hat{\rho}_{DK} | \alpha' \rangle = |\langle \alpha' | \psi_{DK} \rangle|^2 \tag{22}$$

for the displaced Kerr states, using the same parameters as were used to calculate the photon-number distributions in Fig. 3. Although the banana shape of the QPD's for values of γ which correspond to sub-Poissonian statistics is well known, the connection between the shape of the QPD's and that of the number distributions has not been made clear. The QPD for the sub-Poissonian state with $\gamma=0.08$ is shown in Fig. 4(a) and those of the super-Poissonian states with $\gamma=0.2$ and 1.0 are shown in Figs. 4(b) and 4(c). By comparing Fig. 4 with Fig. 3 we see that for a sub-Poissonian state, the QPD lies in the first quadrant and the extra oscillation in the number distribution is to the left of the main curve. For the moderately super-Poissonian state, the QPD lies in the second and third quadrant and the extra oscillations lie to the right of the main peak. For the highly super-Poissonian state, the QPD is ringlike and breaks up into islands, whereas the photon distribution shows no regular pattern.

A qualitative explanation for the shapes of the photon-number distributions can be given by considering the overlap of the QPD for a number state and the displaced Kerr states, as can be seen by expanding the coherent state of Eq. (19) in terms of number states:

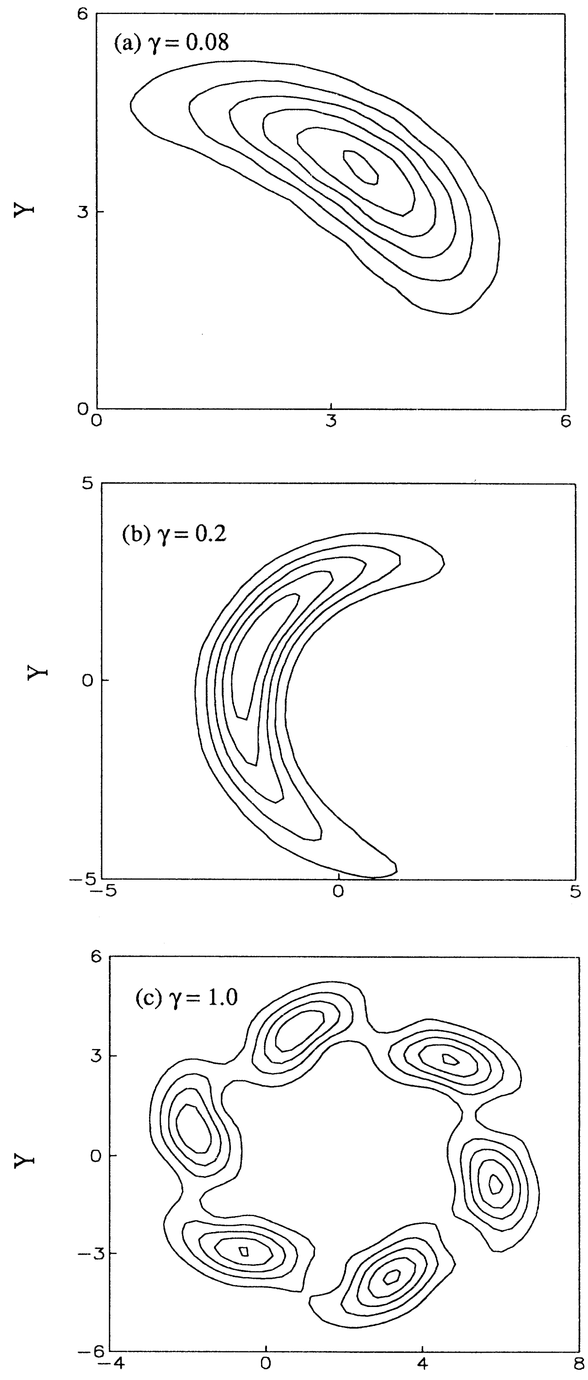

FIG. 4. Quasiprobability distributions for displaced Kerr states for the same parameters as in Figs. 3(a)–3(c). The axes labels are $X \equiv \mathrm{Re}\alpha'$ and $Y \equiv \mathrm{Im}\alpha'$.

$$Q(\alpha')=\left|\sum_{n=0}^{\infty} r_n \langle n|\psi_{DK}\rangle\right|^2 . \tag{23}$$

This point is illustrated schematically in Fig. 5. The number-state phase-space contours can be represented crudely by concentric annuli, each of area $\hbar\omega$ (in appropriate units). The overlap [38–40] of a particular annulus, representing the state $|n\rangle$, with the displaced Kerr state governs the probability of finding n photons in $|\psi_{DK}\rangle$. For many annuli, there is a single overlapping region and a single contribution to the relevant number-state probability. But there are annuli with more than one overlap area and for these the relative phases of each overlap becomes important, for these interfere constructively or destructively to produce oscillations or modulations in the photon-number probabilities. At this point the geometric shape of the phase-space QPD is important, for it governs the nature and extent of these interference oscillations. In Fig. 5(a) the curvature of the QPD in phase space follows to some extent that of the number-state annuli, indicating a potentially sub-Poissonian state; in addition there are two interfering phase-space overlaps on the smallest n annulus indicating interference oscillations in the small-n region before the main peak of the number-state distribution, while on the large-n side of the main peak there is only *one* overlap area and therefore *no* interference oscillations in this region. In Fig. 5(b) we show schematically the situation when the curvature of the QPD in phase space is in the opposite sense to that of the number-state annuli. In this case the situation is reversed and the photon-number oscillations are present on the large-n side of the main peak of the distribution just as in the case of highly quadrature-squeezed coherent light [2,37,38]. We see therefore a simple qualitative explanation of the oscillations visible in Fig. 3.

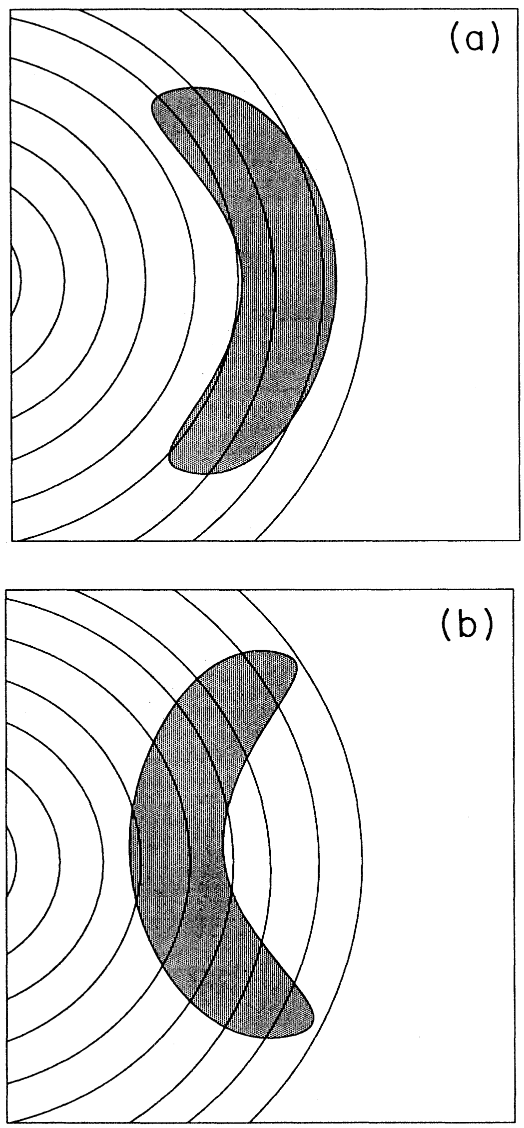

FIG. 5. Illustration of phase-space contours of displaced Kerr states (shaded) overlapping number-state annuli (concentric rings). In (a) the displaced Kerr state is sub-Poissonian, whereas in (b) it is super-Poissonian. Oscillations in the photon-number distributions stemming from interference in phase space occur on the leading or trailing edge of the distribution, respectively.

IV. PHASE-PHOTON-NUMBER UNCERTAINTY RELATION

As pointed out in the Introduction, it is important to use the Pegg-Barnett [21–23] version of the phase-photon-number uncertainty principle when dealing with displaced Kerr states of modest average photon numbers. It will be recalled that in the Pegg-Barnett formalism, the Hermitian phase operator and phase states are defined using a limited basis set consisting of $(s+1)$ number states. After all the calculations are performed, the limit $s\to\infty$ is taken. We shall adopt this view here although we realize [39] that the consistent approach for $s>1$ is to define all *states* and operators for finite s and only at the end of the calculations to take the limit.

The Hermitian phase operator is defined as

$$\hat{\phi}_\theta \equiv \sum_{m=0}^{s} \theta_m |\theta_m\rangle\langle\theta_m| , \tag{24}$$

where the phase states $|\theta_m\rangle$ form a complete orthonormal basis set with

$$\theta_m=\theta_0+\frac{2\pi m}{s+1}, \quad m=0,1,\ldots,s . \tag{25}$$

The choice of the reference phase θ_0 is discussed by Barnett and Pegg [21–23] for large values of the average photon number. We should stress that this is not the limit of central interest to us and we will show later that it is not always possible to choose a reasonable value of θ_0 for small average photon numbers. The number state $|n\rangle$ can be expanded in terms of the θ_m states as

$$\begin{aligned}|n\rangle &= \sum_{m=0}^{s} |\theta_m\rangle\langle\theta_m|n\rangle \\ &=(s+1)^{-1/2}\sum_{m=0}^{s} \exp(-in\theta_m)|\theta_m\rangle . \end{aligned}\tag{26}$$

In order to calculate both sides of the uncertainty relation

$$\langle(\Delta\hat{\phi}_\theta)^2\rangle\langle(\Delta\hat{n})^2\geq\frac{|\langle[\hat{n},\hat{\phi}_\theta]\rangle|^2}{4} \tag{27}$$

for coherent, Kerr, and displaced Kerr states, we first write these states as linear combinations of n-photon states and then use Eqs. (24)–(26) to calculate the relevant matrix elements.

In order to calculate the left-hand side of Eq. (27) for displaced Kerr states, say, we require

$$\langle\psi_{DK}|\hat{\phi}_\theta^t|\psi_{DK}\rangle = \sum_{\substack{nn'\\ n\neq n'}} c_{n'}^* c_n\langle n'|\hat{\phi}_\theta^t|n\rangle+\sum_n |c_n|^2\langle n|\hat{\phi}_\theta^t|n\rangle\ , \quad t=1,2\ . \tag{28}$$

Barnett and Pegg have shown that in the limit $s\to\infty$

$$\langle n|\hat{\phi}_\theta|n\rangle\simeq\theta_0+\pi\ , \tag{29}$$

$$\langle n'|\hat{\phi}_\theta|n\rangle\simeq\frac{i}{n-n'}e^{i(n'-n)\theta_0},\quad n\neq n' \tag{30}$$

$$\langle n|\hat{\phi}_\theta^2|n\rangle\simeq\theta_0^2+2\pi\theta_0+\frac{4\pi^2}{3}\ , \tag{31}$$

and one can show that

$$\langle n'|\hat{\phi}_\theta^2|n\rangle\simeq\left[\frac{2i\theta_0}{n-n'}+\frac{2i\pi}{n-n'}+\frac{2}{(n-n')^2}\right]e^{i(n'-n)\theta_0}\ , \quad n\neq n' \tag{32}$$

using [41]

$$\sum_{m=0}^{s} d^m=0\ ,$$
$$\sum_{m=0}^{s} md^m=\frac{s+1}{d-1}\ , \tag{33}$$
$$\sum_{m=0}^{s} m^2d^m=\frac{s+1}{(d-1)^2}[(s-1)(d-1)-2]$$

and

$$\lim_{s\to\infty}(s\pm1)(d-1)=i(n'-n)2\pi\ , \tag{34}$$

where

$$d\equiv\exp[i(n'-n)2\pi/(s+1)]\ . \tag{35}$$

With the help of Eqs. (29)–(32), one finds from Eq. (28) that in the limit $s\to\infty$

$$\langle\psi_{DK}|\hat{\phi}_\theta|\psi_{DK}\rangle=(\theta_0+\pi)+i\sum_{\substack{n,n',\\ n!=n'}}\frac{c_{n'}^*c_n}{(n-n')}e^{i(n'-n)\theta_0} \tag{36}$$

and

$$\langle\psi_{DK}|\hat{\phi}_\theta^2|\psi_{DK}\rangle=(\theta_0^2+2\pi\theta_0+4\pi^2/3)+2\sum_{\substack{n,n',\\ n\neq n'}}\frac{c_{n'}^*c_n}{(n-n')}\times\left[i(\theta_0+\pi)+\frac{1}{(n-n')}\right]\times e^{i(n'-n)\theta_0}\ . \tag{37}$$

In order to calculate the right-hand side of Eq. (27) we write

$$\langle\psi_{DK}|[\hat{n},\hat{\phi}_\theta]|\psi_{DK}\rangle=\sum_{nn'}c_{n'}^*c_n\langle n'|[\hat{n},\hat{\phi}_\theta]|n\rangle \tag{38}$$

and use the result

$$\langle n'|[\hat{n},\hat{\phi}_\theta]|n\rangle\simeq-i(1-\delta_{n'n})e^{i(n'-n)\theta_0}\ ,\quad s\to\infty \tag{39}$$

to obtain

$$\langle\psi_{DK}|[\hat{n},\hat{\phi}_\theta]|\psi_{DK}\rangle\simeq-i\sum_{\substack{n,n',\\ n\neq n'}}c_{n'}^*c_n e^{i(n'-n)\theta_0}\ , \tag{40}$$

which is a c number.

Obviously, the above method can be used for any state of the field that can be written as a linear superposition of n-photon states. We shall present calculations for coherent states, Kerr states, and displaced Kerr states for moderate average photon numbers.

Another method of calculating the phase-photon-number uncertainty relation has been used for *large* average photon numbers when the field exhibits Poissonian statistics. The method involves writing [compare Eq. (28)]

$$\langle\alpha|\hat{\phi}_\theta^t|\alpha\rangle=\sum_{m=0}^{s}|\langle\alpha|\theta_m\rangle|^2\theta_m^t \equiv\sum_{m=0}^{s}P_{\theta_m}\theta_m^t,\quad t=1,2 \tag{41}$$

and then invoking Eqs. (7) and (26) to express $|\alpha\rangle$ and $|\theta_m\rangle$ in terms of the number states $|n\rangle$. The amplitudes $r_n\equiv\langle n|\alpha\rangle$ are then replaced, apart from the appropriate phase factor, by the square root of a continuous Gaussian distribution. The summation over n that appears in the calculation of $\langle\alpha|\theta_m\rangle$ is replaced by an integral. The resulting phase probability distribution $P_{\theta_m}\equiv P(\theta)$ is now a continuous function of θ_m and the summation over m in Eq. (38) is replaced by an integral so that

$$\langle\alpha|\hat{\phi}_\theta^t|\alpha\rangle=\int_{\theta_0}^{\theta_0+2\pi}P(\theta)\theta^t d\theta,\quad t=1,2\ . \tag{42}$$

When θ_0 is chosen to be sufficiently far from the maximum of $P(\theta)$, it is found that

$$\langle\Delta\hat{\phi}_\theta^2\rangle=\frac{1}{4|\alpha|^2}=\frac{1}{4\bar{n}}\ , \tag{43}$$

in agreement with the phenomenological result. This method is obviously unsuited to photon-number distribu-

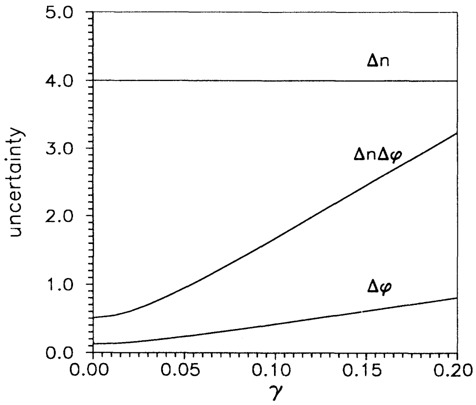

FIG. 6. Phase and photon-number variances $\Delta\varphi$ and Δn, and their product for a Kerr state with $|\alpha|=4$, $\phi_\alpha=0$ vs γ. For $\gamma<0.01$, $\Delta n\Delta\varphi=\frac{1}{2}$ and so the Kerr state is a MUS.

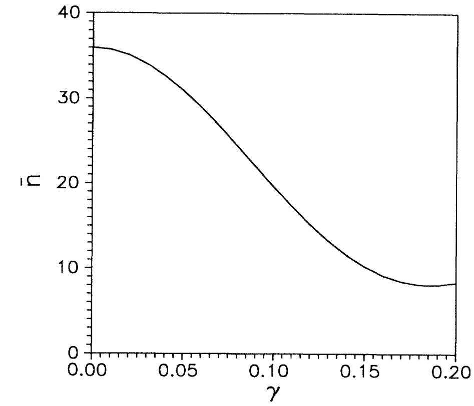

FIG. 8. Mean photon number n vs γ for a displaced Kerr state with $|\alpha|=4$, $|\xi|=2$, and $\phi_\alpha=\phi_\xi=0$.

tions which cannot be approximated by a continuous function. Nevertheless, it is interesting to compare the results obtained for coherent and Kerr states with those obtained by our summation procedure.

In our calculations we choose θ_0 to be well outside the region of phase space occupied by the QPD, $Q(\alpha')$. As long as this condition is respected, the left-hand side of the uncertainty relation has the same numerical value for a large range of values of θ_0 and the right-hand side is equal to $\frac{1}{4}$. It is obvious from Fig. 4 that as the region occupied by the QPD changes with γ, the range of values of θ_0 will also change and for high values of γ (or low values of $|\alpha+\xi|$), both sides of Eq. (27) will be θ_0 dependent. This procedure for choosing θ_0 is equivalent to that of taking θ_0 to be far from the maximum of the $P(\theta)$ distribution.

In Figs. 6 and 7 we plot $\Delta n\equiv\langle\Delta n^2\rangle^{1/2}$, $\Delta\varphi\equiv\langle\Delta\phi_\theta^2\rangle^{1/2}$, and $\Delta n\Delta\varphi$ for Kerr and displaced Kerr states, respectively, as a function of γ. In both cases, we find for $\gamma=0$, that, as expected, $\Delta\varphi^2>(1/4\bar{n})$ so that

$$\Delta\varphi\Delta n>\tfrac{1}{2}\ . \tag{44}$$

For example, for $|\alpha|=4$, $1/4\bar{n}=\frac{1}{64}$ and $\Delta\varphi^2=\frac{1}{62}$ (Fig. 6). The deviation of $\Delta\varphi^2$ from $1/4\bar{n}$ decreases as n increases as one would expect. Thus the phenomenological result is only strictly true for large values of $\bar{n}$. The Kerr states in Fig. 6 are only (MUS's) for $\gamma\lesssim0.01$. This is due to the fact that $\Delta\varphi$ increases steadily with γ and Δn is of course constant. This is in contrast to the displaced Kerr states (see Fig. 7) where the increase in $\Delta\varphi$ with γ is compensated by a decrease in Δn so that the states are MUS's for $\gamma\lesssim0.08$. Thus there is a range of parameters $0.8\lesssim\gamma\lesssim0.13$ where the displaced Kerr states deviate from minimum uncertainty but still retain sub-Poissonian statistics. It should be noted that the range for which $Q<0$ (see Fig. 2) does not correspond to the range for which $\Delta n<|\alpha+\xi|$. This is due to the fact that Q is determined by both Δn and n, and n also varies with γ. In fact, as can be seen from Fig. 8, n decreases with increasing γ until about $\gamma\simeq0.18$.

We now choose the value of γ ($\gamma=0.08$) that gives the

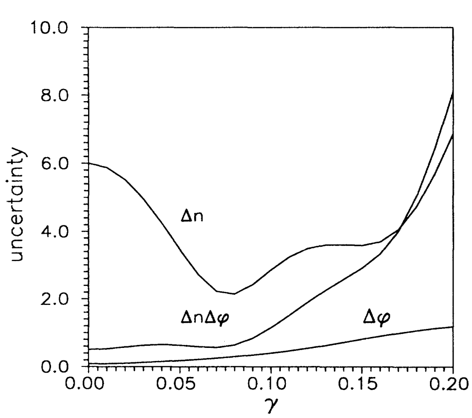

FIG. 7. Phase and photon-number variances, $\Delta\varphi$ and Δn, and their product for a displaced Kerr state with $|\alpha|=4$, $|\xi|=2$, and $\phi_\alpha=\phi_\xi=0$. For $\gamma<0.8$, $\Delta n\Delta\varphi=\frac{1}{2}$ and so the displaced Kerr state is a MUS.

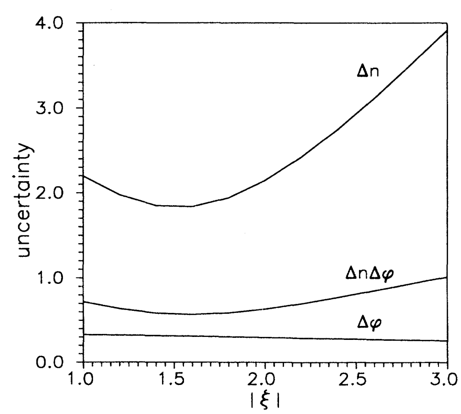

FIG. 9. Phase and photon-number variances, $\Delta\varphi$ and Δn, and their product vs $|\xi|$ for a displaced Kerr state with $|\alpha|=4$, $\phi_\alpha=\phi_\xi=0$, and the value of γ ($\gamma=0.08$) that gives the minimum value of Q for $|\xi|=2$. We see that the displaced Kerr state is close to a MUS over the whole range of $|\xi|$ shown.

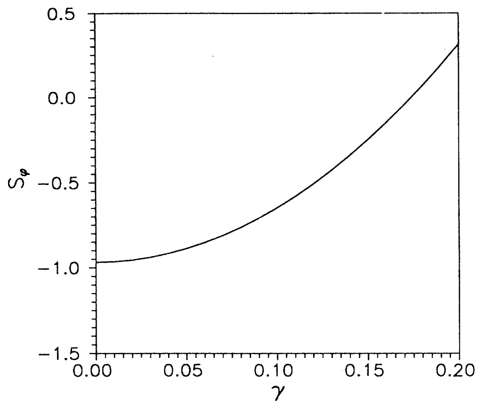

FIG. 10. Phase-squeezing parameter S_φ vs γ for a Kerr state with $|\alpha|=4$, $\phi_\alpha=0$.

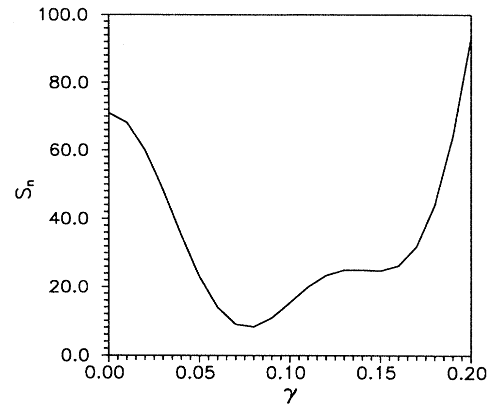

FIG. 12. Photon-number squeezing parameter S_φ vs γ for a displaced Kerr state with $|\alpha|=4$, $|\xi|=2$, and $\phi_\alpha=\phi_\xi=0$.

greatest degree of sub-Poissonian statistics for $|\alpha|=4$, $|\xi|=2$, and plot Δn, $\Delta\varphi$, and $\Delta n\Delta\varphi$ as a function of $|\xi|$ for $|\alpha|=4$ and $\gamma=0.08$ in Fig. 9. We see that $\Delta\varphi$ does not change markedly with $|\xi|$ so that the product $\Delta n\Delta\varphi$ is determined for the most part by Δn. We see that for $1\le|\xi|\le3$, the displaced Kerr states, although not precisely MUS's, do not deviate strongly from minimum uncertainty.

Following Wódkiewicz and Eberly [42], we can say that the number or phase fluctuations are squeezed if

$$\langle \Delta\hat{\varphi}_\theta^2\rangle < \tfrac{1}{2}|\langle[\hat{n},\hat{\phi}_\theta]\rangle| \,, \tag{45}$$

or

$$\langle \Delta\hat{n}^2\rangle < \tfrac{1}{2}|\langle[\hat{n},\hat{\phi}_\theta]\rangle| \,. \tag{46}$$

A measure of the squeezing was suggested previously [39] by introducing the parameters

$$S_\varphi=\frac{\langle \Delta\hat{\varphi}_\theta^2\rangle-\frac{1}{2}|\langle[\hat{n},\hat{\varphi}_\theta]\rangle|}{\frac{1}{2}|\langle[\hat{n},\hat{\varphi}_\theta]\rangle|} \,, \tag{47}$$

$$S_n=\frac{\langle \Delta\hat{n}^2\rangle-\frac{1}{2}|\langle[\hat{n},\hat{\varphi}_\theta]\rangle|}{\frac{1}{2}|\langle[\hat{n},\hat{\varphi}_\theta]\rangle|} \,. \tag{48}$$

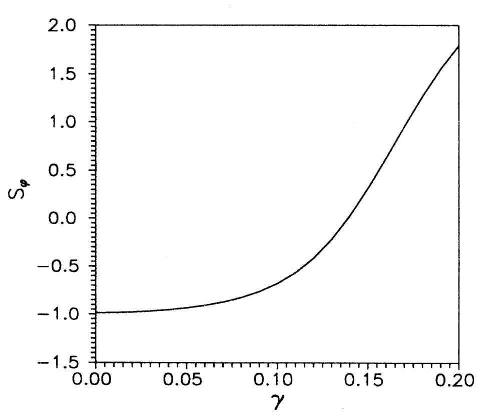

FIG. 11. Phase-squeezing parameter S_φ vs γ for a displaced Kerr state with $|\alpha|=4$, $|\xi|=2$, and $\phi_\alpha=\phi_\xi=0$.

Maximum squeezing corresponds to $S_\varphi=-1$ or $S_n=-1$. We first calculate these squeezing parameters as a function of γ for Kerr states and for displaced Kerr states. Figure 10 shows S_φ vs γ for Kerr states and Fig. 11 shows S_φ for displaced Kerr states. Following the terminology of Glauber and Lewenstein [43], we can say that the phase is subfluctuant for $0\le\gamma\lesssim0.17$ for the Kerr states and for $0\le\gamma\le0.13$ in the case of displaced Kerr states. Because the Kerr states are Poissonian, S_n is a constant in that case ($S_n=31$ for $|\alpha|=4$), and S_n as a function of γ is shown in Fig. 12 for the displaced Kerr states. We see that $S_n>0$, so that the photon number is superfluctuant for all values of γ. Thus according to the present definition, the *phase* is squeezed whereas the photon number is not. We see therefore that the concept of a sub-Poissonian statistics ($Q<0$) is not equivalent to that of photon-number squeezing [if defined as in Eq. (48)].

V. QUADRATURE SQUEEZING

In the same way as we defined the degree of squeezing for the phase and photon number, we can define $S_{1,2}$, the degree of squeezing for the quadrature operators which are linear combinations of the photon creation and annihilation operators,

$$\hat{a}_1=\frac{\hat{a}+\hat{a}^\dagger}{2}, \quad \hat{a}_2=\frac{\hat{a}-\hat{a}^\dagger}{2i} \,. \tag{49}$$

Thus

$$S_{1,2}=4[\langle(\Delta\hat{a}_i)^2\rangle-\tfrac{1}{4}] \tag{50}$$

since $|[\hat{a}_1,\hat{a}_2]|=\frac{1}{2}$. Substituting (49) into (50), we find that

$$S_1=2\langle\hat{n}\rangle+2\,\mathrm{Re}\langle\hat{a}^2\rangle-4\,\mathrm{Re}(\langle\hat{a}\rangle)^2 \,, \tag{51}$$

$$S_2=2\langle\hat{n}\rangle-2\,\mathrm{Re}\langle\hat{a}^2\rangle-4\,\mathrm{Im}(\langle\hat{a}\rangle)^2 \,, \tag{52}$$

where

$$\langle\hat{a}\rangle=\sum_{n=0}^{\infty} c_n^* c_{n+1}(n+1)^{1/2} \tag{53}$$

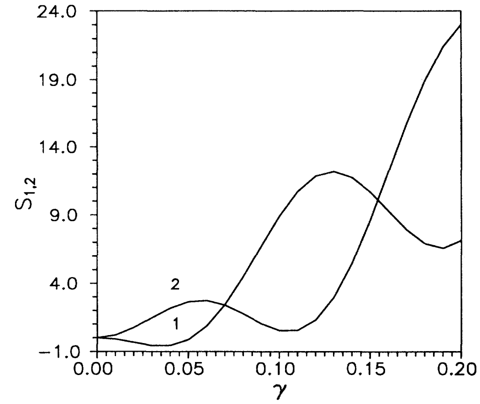

FIG. 13. Quadrature squeezing parameters $S_{1,2}$ vs γ for a Kerr state with $|\alpha|=4$, $\phi_\alpha=0$.

and

$$\langle \hat{a}^2 \rangle = \sum_{n=0}^{\infty} c_n^* c_{n+2}[(n+1)(n+2)]^{1/2} \qquad (54)$$

for displaced Kerr states and similar expressions with c's replaced by q's for the Kerr states. As may be expected physically the degree of quadrature squeezing is independent of $|\xi|$: displacing a QPD in phase space does not alter its degree of quadratic squeezing. We plot $S_{1,2}$ as a function of γ in Fig. 13 and observe that squeezing is obtained for $0 \le \gamma \lesssim 0.05$ with a maximum degree of quadrature squeezing of $S_1 = -0.6$. Thus there exists a range of parameters for which the sub-Poissonian statistics and quadrature squeezing can coexist ($0 \le \gamma \lesssim 0.05$ for $|\alpha|=4$, $|\xi|=2$).

VI. CONCLUSIONS

We have studied the statistical and phase properties of the output states of a Mach-Zehnder interferometer with a nonlinear Kerr medium in one of its arms. We found that the combination of nonlinearity and displacement produced by the interferometer generates output states (displaced Kerr states) which, unlike those generated by the Kerr medium along (Kerr states), do not necessarily retain the Poissonian statistics of the input coherent field. We found for small photon numbers that as the parameter γ characterizing the nonlinear Kerr medium is varied, the statistics of the output field as determined by the Mandel Q parameter range from sub-Poissonian to super-Poissonian. The photon-number distribution of a sub-Poissonian state is characterized by a small peak to lower photon number of the main narrow peak, whereas that of a moderately super-Poissonian state exhibits interference peaks of decreasing amplitude to the higher-photon-number side of the main peak. The photon-number distribution of a highly super-Poissonian state has no discernable pattern. These characteristic features have been rationalized by examining the overlap of the appropriate QPD's with those of the n-photon states. The QPD's of the displaced Kerr states vary from bananalike for sub-Poissonian states to ringlike with a complicated interference structure for highly super-Poissonian states.

The number-phase properties of both the Kerr and displaced Kerr states have been studied for small photon numbers using a methodology based on the Pegg-Barnett formalism but taking account of the discrete nature of the phase distribution for low photon numbers. We have determined the range of parameters for which the Kerr and displaced Kerr states are MUS's and have shown the coherent states approach MUS's with increasing photon number. We have investigated the squeezing with respect to number and phase of the Kerr and displaced Kerr states, clarifying the distinction between a sub-Poissonian nature and number squeezing. Finally, we found that quadrature squeezing which is independent of the displacement can coexist for a range of parameters with sub-Poissonian statistics.

ACKNOWLEDGMENT

This work was supported in part by the U.K. Science and Engineering Research Council.

*Permanent address: Department of Chemistry, Bar-Il an University, Ramat-Gan 59100, Israel.

†Permanent address: Institute of Physics, Slovak Academy of Sciences, Dúbravská cesta 9, 84228 Bratislava, Czechoslovakia.

[1] R. Loudon and P. L. Knight, J. Mod. Opt. **34**, 709 (1987).
[2] K. Zaheer and M. S. Zubairy, in *Advances in Atomic Molecular and Optical Physics,* edited by D. Bates and B. Bederson (Academic, New York, 1990), Vol. 28, p. 143.
[3] M. C. Teich and B. E. A. Saleh, Quantum Opt. **1**, 153 (1989).
[4] L. Mandel, Phys. Scr. **T12**, 34 (1986).
[5] L. Mandel, Phys. Rev. Lett. **49**, 136 (1982); **51**, 384 (1983).
[6] P. N. Butcher and D. Cotter, *The Elements of Nonlinear Optics* (Cambridge University Press, Cambridge, 1990).
[7] R. Tanaś, in *Coherence and Quantum Optics V,* edited by L. Mandel and E. Wolf (Plenum, New York, 1984), p. 645.
[8] B. Yurke and D. Stoler, Phys. Rev. Lett. **57**, 13 (1986).
[9] P. Tombesi and A. Mecozzi, J. Opt. Soc. Am. B **4**, 1700 (1987).
[10] G. J. Milburn, Phys. Rev. A **33**, 674 (1986).
[11] G. J. Milburn and C. A. Holmes, Phys. Rev. Lett. **56**, 2237 (1986).
[12] A. Miranowicz, R. Tanaś, and S. Kielich, Quantum Opt. **2**, 253 (1990).
[13] See, for instance, *Quantum Measurement in Optics,* edited by P. Tombesi (Plenum, New York, in press).
[14] W. H. Louisell, *Quantum Statistical Properties of Radiation* (Wiley, New York, 1973).
[15] H. H. Ritze and A. Bandilla, Opt. Commun. **29**, 126 (1979).
[16] M. Kitagawa and Y. Yamamoto, Phys. Rev. A **34**, 3974 (1986).
[17] N. Imoto, H. A. Haus, and Y. Yamamoto, Phys. Rev. A

32, 2287 (1985).
[18] Y. Yamamoto and H. Haus, Rev. Mod. Phys. **58**, 1001 (1986).
[19] M. Shirasaki and H. A. Haus, J. Opt. Soc. Am. B **7**, 30 (1990).
[20] M. Shirasaki, Opt. Lett. **16**, 171 (1991).
[21] D. T. Pegg and S. M. Barnett, Europhys. Lett. **6**, 483 (1988).
[22] D. T. Pegg and S. M. Barnett, Phys. Rev. A **39**, 1665 (1989).
[23] S. M. Barnett and D. T. Pegg, J. Mod. Opt. **36**, 7 (1989).
[24] D. Meschede, H. Walther, and G. Müller, Phys. Rev. Lett. **54**, 551 (1985).
[25] G. Rempe, H. Walther, and N. Klein, Phys. Rev. Lett. **58**, 353 (1987).
[26] G. Rempe, W. Schleich, M. O. Scully, and H. Walther, in Proceedings of the Third International Symposium on Foundations of Quantum Mechanics (Physical Society of Japan, Tokyo, 1989), p. 294.
[27] H. Moya-Cessa, V. Bužek, and P. L. Knight, Opt. Commun. **85**, 267 (1991).
[28] M. Brune, J. M. Raimond, P. Goy, L. Davidovich, and S. Haroche, IEEE J. Quantum Electron **24**, 1323 (1988), and references therein.
[29] W. K. Lai, V. Bužek, and P. L. Knight, Phys. Rev. A **44**, 6043 (1991).
[30] M. Brune, S. Haroche, V. Lefevre, J. M. Raimond, and N. Zagury, Phys. Rev. Lett. **65**, 976 (1990).
[31] L. Susskind and J. Glogower, Physics **1**, 49 (1964).
[32] P. Carruthers and M. H. Nieto, Rev. Mod. Phys. **40**, 411 (1968).
[33] C. C. Gerry, Opt. Commun. **77**, 168 (1990).
[34] H. Fearn and R. Loudon, Opt. Commun. **64**, 485 (1987).
[35] S. M. Roy, V. Singh, Phys. Rev. D **25**, 3413 (1982).
[36] F. A. M. de Oliveira, M. S. Kim, P. L. Knight, and V. Bužek, Phys. Rev. A **41**, 2645 (1990), and references therein.
[37] F. A. M. de Oliveira, P. L. Knight, G. M. Palma, and A. K. Ekert, in *Noise and Chaos in Nonlinear Dynamical Systems,* edited by F. Moss, L. Lugiato and W. Schleich (Cambridge University Press, Cambridge, 1990).
[38] W. Schleich and J. A. Wheeler, J. Opt. Soc. Am. B **4**, 1715 (1987).
[39] V. Bužek, A. D. Wilson-Gordon, P. L. Knight, and W. K. Lai (unpublished).
[40] J. A. Wheeler, Lett. Math. Phys. **20**, 201 (1985); W. Schleich and J. A. Wheeler, Nature **326**, 574 (1987).
[41] I. S. Gradshteyn and I. M. Ryzhik, *Tables of Integrals, Series and Products* (Academic, San Diego, 1980).
[42] K. Wódkiewicz and J. H. Eberly, J. Opt. Soc. Am. B **2**, 458 (1985).
[43] R. J. Glauber and M. Lewenstein, Phys. Rev. A **43**, 467 (1991).